Available online at www.sciencedirect.com
SCIENCE DIRECT
Journal of Solid State Chemistry 179 (2006) 2386–2393
JOURNAL OF SOLID STATE CHEMISTRY
www.elsevier.com/locate/jssc

Anion mediated polytype selectivity among the basic salts of Co(II)

T.N. Ramesh[a], Michael Rajamathi[b], P. Vishnu Kamath[a,*]

[a]Department of Chemistry, Central College, Bangalore University, Bangalore 560 001, India
[b]Department of Chemistry, St. Joseph's College, Lalbagh Road, Bangalore 560 027, India

Received 4 February 2006; received in revised form 23 April 2006; accepted 27 April 2006
Available online 12 May 2006

Abstract

Basic salts of Co(II) crystallize in the rhombohedral structure. Two different polytypes, $3R_1$ and $3R_2$, with distinct stacking sequences of the metal hydroxide slabs, are possible within the rhombohedral structure. These polytypes are generated by simple translation of successive layers by (2/3, 1/3, z) or (1/3, 2/3, z). The symmetry of the anion and the mode of coordination influences polytype selection. Cobalt hydroxynitrate crystallizes in the structure of the $3R_2$ polytype while the hydroxytartarate, hydroxychloride and α-cobalt hydroxide crystallize in the structure of the $3R_1$ polytype. Cobalt hydroxysulfate is turbostratically disordered. The turbostratic disorder is a direct consequence of the mismatch between the crystallographically defined interlayer sites generated within the crystal and the tetrahedral symmetry of the SO_4^{2-} ions.

Keywords: Cobalt hydroxysalts; DIFFaX simulations; Polytypes; Urea hydrolysis

1. Introduction

In the class of layered compounds, divalent metal hydroxides crystallize in the structure of mineral brucite, $Mg(OH)_2$. Brucite comprises a hexagonal close packing of hydroxyl ions with alternate layers of octahedral sites occupied by divalent metal ions. This results in the stacking of charge-neutral layers of composition $[M(OH)_2]$ (M = Mg, Co, Ni) with an interlayer distance of ≈4.7 Å [1]. Layered hydroxysalts (basic salts) [2] also derive their structure from brucite and comprise a stacking of hydroxyl deficient positively charged layers having the composition $[M(OH)_{2-x}]^{x+}$. The structure incorporates anions ($A^{n-} = Cl^-$, NO_3^-, SO_4^{2-}, CO_3^{2-}) in the interlayer region to restore charge neutrality yielding compounds with the general formula $[M(OH)_{2-x}](A^{n-})_{x/n}$. The commonly observed values of x are 0.5, 0.67 and 1.0. Compositionally these represent a series of solid solutions whose end members are $M(OH)_2$ and M_nA_2. Structurally the hydroxyl-rich phases ($x = 0.5$, 0.67) adopt structures isotypic with mineral brucite, while the anion-rich phases ($x \geqslant 1$) adopt a structure of lower symmetry. In all these compounds the M^{2+} ion occupies octahedral sites. The coordinative unsaturation of the metal ions is satisfied by the anions, which are grafted directly to the metal ion. The interlayer spacing is determined by the size of the anion and commonly varies from 6.9 to 9.2 Å [3,4]. Basic salts of the formula $M(OH)A$, $M_3(OH)_4A_2$, and $M_2(OH)_3A$ [$A = Cl^-$, NO_3^-], where $x = 1$, 0.67 and 0.5, respectively, are reported [5–7].

The most common phases reported in the cobalt system are $Co_2(OH)_3NO_3 \cdot 0.25H_2O$ ($x = 0.5$) and $Co_7(OH)_{12}(NO_3)_2 \cdot 5H_2O$ [8]. The former is a single layered hexagonal compound with the cell dimensions $a = 3.17$ and $c = 6.95$ Å, in which all the Co^{2+} ions occupy octahedral sites in brucite-derived layers. The latter structure ($a = 3.13$ and $c = 9.18$ Å) has 5/7 of the Co^{2+} ions in octahedral sites in a brucite-derived layer of the composition $[Co_5(OH)_{12}]$, while the remaining 2/7 occupy tetrahedral sites above and below the layer, leading to an increased c-parameter. $Co(OH)(NO_3) \cdot H_2O$ ($x = 1$) has also been synthesized in both ordered and disordered forms by hydrolysis of Co(II) nitrate melts [9]. This compound is monoclinic ($a = 17.757$ Å; $b = 3.142$ Å; $c = 14.188$ Å; $\beta = 113.55°$) and isostructural with $Zn(OH)(NO_3) \cdot H_2O$ and consists of infinite double octahedral chains running parallel to the [010]

*Corresponding author.
E-mail address: vishnukamath8@hotmail.com (P. Vishnu Kamath).

0022-4596/$ - see front matter © 2006 Elsevier Inc. All rights reserved.
doi:10.1016/j.jssc.2006.04.034

direction [10]. Rajamathi and Kamath [11] reported the basic salt of Co with the composition $Co_3(OH)_4(NO_3)_2$ ($x = 0.67$) having a hexagonal structure similar to its Ni analog.

The structure of $M_2(OH)_3Cl$ (M = Co, Cu) comprises a close packing of $(OH)_3Cl$ in which M^{2+} occupies the octahedral sites. In such structures, the metal ion is surrounded by $4OH^-$ and $2Cl^-$ ions to form octahedral coordination. The crystal structure is driven by the nature of M^{2+} ion. $Cu_2(OH)_3Cl$ crystallizes in the structure of mineral atacamite which is not layered, while $Co_2(OH)_3Cl$ crystallizes with rhombohedral symmetry [12]. $Zn_5(OH)_8Cl_2$ ($a = 6.34$ Å; $c = 23.64$ Å) has a structure similar to that of $Co_7(OH)_{12}(NO_3)_2$ with Zn^{2+} in both octahedral and tetrahedral sites [13].

Among layered compounds, more important than the exact crystal structure is the stacking sequence of the hydroxyl ions. The structural anisotropy of layered compounds often permits them to crystallize in different structures that vary in the way the metal hydroxide slabs are stacked—a phenomenon known as polytypism [14]. Polytypism is a 1-D polymorphism in which, structural changes manifest exclusively along the stacking direction. The study of different polytypes is a subject of contemporary interest in the chemistry of layered materials [15,16]. When different polytypes have very similar thermodynamic stabilities, they tend to intergrow randomly to produce crystals with stacking disorders [17].

Basic salts are model layered compounds, which despite their structural simplicity typified by the presence of a single metal ion in octahedral sites, have the functional ability to undergo anion exchange reactions [18]. As a part of our continuing interest in the study of polytypism and stacking disorders in layered hydroxides [19,20], in this paper, we examine the phenomenon of polytypism among the basic salts of Co(II) and demonstrate how different anions select for different polytypes by mediating the stacking of metal hydroxide slabs—a phenomenon having all the characteristics of molecular recognition.

2. Experimental section

The basic salts of Co(II) were synthesized by urea hydrolysis of the corresponding molten salts of Co(II) at 140 ± 3 °C in an open glass beaker. In a typical synthesis, 18 g of CoA_2 ($A = Cl^-$, NO_3^-) was mixed with 2 g of urea and 2 mL of water in a beaker and the mixture was placed inside a pre-heated air oven. It was occasionally stirred until it turned viscous at which stage the mixture was removed from the oven and cooled to room temperature. The hard cake obtained was ground in water, filtered and washed until the washings were free from Co^{2+} ions. Then it was washed with acetone and dried at room temperature to constant weight [11].

Anion exchange reactions were carried out by suspending 0.5 g of the cobalt hydroxynitrate in:

(a) 67 mL of 0.25 M sodium potassium tartarate buffer (pH 7.3) for 5 days at the ambient temperature (23–25 °C). At the end of the exchange process the supernatant was pink and the solid turned gray. The sample after exchange was filtered in a sintered glass crucible, washed with water and then with acetone, dried to constant weight at 65 °C.

(b) 108 mL of 0.25 M sodium chloride (pH 7) for 5 days at the ambient temperature (23–25 °C). The green solid after exchange was separated by centrifugation, washed with water and then with acetone prior to drying at 65 °C till constant weight is attained.

All samples were characterized by powder X-ray diffraction (PXRD) using a Philips powder X-ray diffractometer (Cu$K\alpha$ source, $\lambda = 1.541$ Å) fitted with a graphite monochromator. Data were collected at a scan rate of 2° $2\theta\,min^{-1}$ and rebinned into 2θ steps of 0.02°. Infrared spectra were recorded using a Nicolet Model Impact 400D FTIR spectrometer (KBr pellets, $4\,cm^{-1}$ resolution). Thermogravimetry was carried out using a Mettler Toledo Model 851^e TG/SDTA system (heating rate $5\,°C\,min^{-1}$). All the samples were heated to 100 °C for 30 min, and the weight loss was accounted from 100 to 800 °C.

All the samples were subjected to wet chemical analysis. The Co content was determined by weighing the product of thermal decomposition (800 °C) as Co_3O_4 ($a = 8.08$ Å). The hydroxyl content was determined by reacting a known weight of the sample with an excess of standard HCl and back-titrating the excess acid with standard NaOH using a pH meter. As expected, the [Co]/[OH^-] ratio was found to be >0.5 showing that the metal hydroxide slabs are hydroxyl-deficient. The hydroxyl deficiency was compensated by the inclusion of anions. The Cl^- and SO_4^{2-} content was also independently estimated gravimetrically as AgCl and $BaSO_4$, respectively. These estimations were found to match with the hydroxyl ion deficiency. The unaccounted weight was attributed to intercalated water. The approximate formulae obtained from these data were verified by the net losses observed from isothermal decomposition ($T = 800$ °C). The results of wet chemical analysis are given in Table 1.

3. DIFFaX simulations

The DIFFaX code [21] enables the simulation of the PXRD pattern of a crystalline material. Within the DIFFaX formalism, a crystalline solid is treated as a stacking of layers of atoms and the diffraction intensities are computed layer by layer and integrated over a infinite or finite number of layers. This formalism enables us to build in different stacking sequences to generate the PXRD patterns of different polytypes. DIFFaX has been used successfully to study polytypism and disorder among the layered hydroxides [22–24]. The various details used in the simulation are given below:

(a) The cell parameters of each basic salt were obtained by indexing the corresponding PXRD pattern.

Table 1
Chemical composition of various hydroxysalts of Co(II)

Anion	Weight percentage				Isothermal weight loss (%)[a]	Approximate formula
	Co	OH	A^{n-}	H_2O		
Nitrate	49.4	19.4	31.2	—	33.5 (34.0)	$Co(OH)_{1.36}(NO_3)_{0.64}$
Tartarate	39.7	18.9	25.7	15.67	39.3 (39.5)	$Co(OH)_{1.65}(C_6H_4O_6)_{0.17}\cdot 0.87H_2O$
Chloride	56.4	24.0	18.8[b]	—	23.1 (22.6)	$Co(OH)_{1.47}(Cl)_{0.55}$
Sulphate	50.1	23.7	14.4[b]	9.15	31.6 (31.2)	$Co(OH)_{1.63}(SO_4)_{0.17}\cdot 0.5H_2O$
α-Hydroxide	53.8	27.7	12.0	12.09	26.7 (22.8)	$Co(OH)_{1.78}(Cl)_{0.22}\cdot 0.39H_2O$

[a]Values in parentheses are calculated based on the approximate formula.
[b]Results of independent estimation.

(b) Since the single crystal structure data of cobalt hydroxynitrate was not available, the position parameters of the atoms were taken from the ICSD (88940) data of brucite-like β-$Co(OH)_2$ [Co (0,0,0); O1 (0.6667, 0.3333, *z*); O2 (−0.6667, −0.3333, −*z*)]. The *z*-parameters of the O atoms in each basic salt were chosen in such a way as to reproduce the Co–O bond distance found in β-$Co(OH)_2$. The presence of intercalated species was ignored for the purpose of simulation, as the intercalated species are known to contribute marginally to the diffraction intensity [25]. In the case of $Co_2(OH)_3Cl$, the atom positions were taken from the single crystal data (ICSD No. 24685). The point group symmetry of the solid was declared as unknown and all the symmetry related atoms were explicitly listed. Under this option, the DIFFaX program computes the diffraction symmetry of the solid.

(c) The crystal lattice was defined by stacking the layers described in (b) above, one over another. The use of the stacking vector (0,0,1) yields the 1H polytype. To generate the 2H polytypes two different layers were used. For instance, to generate the $2H_2$ polytype two different layers, AC and AB were defined and stacked one on top of another by using the stacking vector (0,0,1). The stacking probabilities $P_{ACAC} = P_{ABAB} = 0$ and $P_{ACAB} = P_{ABAC} = 1$ simulate the pure $2H_2$ polytype. The $2H_1$ polytype is similarly generated by defining AC and CA layers. The $2H_3$ polytype is generated by defining AC and BA layers. To generate the 3R polytypes, three layers AC, BA and CB were defined and stacked one on top of another by using the stacking vector (0,0,1). The probabilities $P_{ACAC} = P_{BABA} = P_{CBCB} = P_{ACCB} = P_{BAAC} = P_{CBBA}$ were set to zero, while $P_{ACBA} = P_{BACB} = P_{CBAC} = 1$ yield the pure $3R_2$ polytype. To generate the $3R_1$ polytype the probability selection was reversed by setting $P_{ACCB} = P_{BAAC} = P_{CBBA} = 1$.

(d) The calculated Bragg maxima, were broadened by using a Lorentzian line shape function to facilitate comparison with the observed patterns. As DIFFaX is not a profile refinement program and only enables a qualitative comparison of the experimental and calculated patterns, the use of a Lorentzian profile function is adequate. The full-width at half-maxima (FWHM) values of the Lorentzian is chosen to be the same as that of the peak due to the *1 1 0* reflection for all computations.

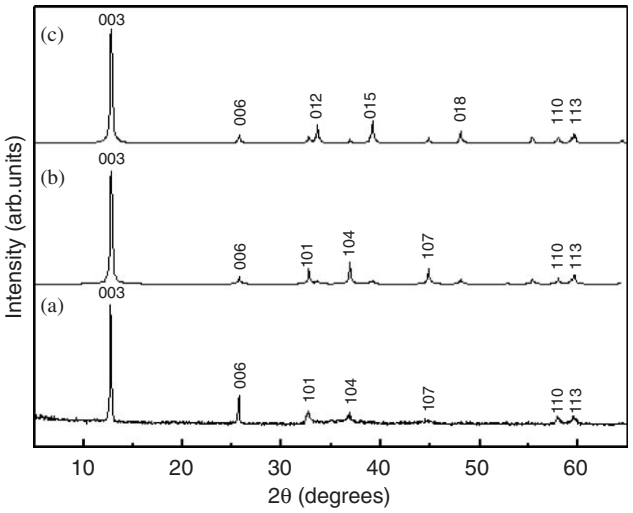

Fig. 1. (a) Observed PXRD pattern of cobalt hydroxynitrate compared with the DIFFaX simulated patterns of (b) $3R_2$ and (c) $3R_1$ polytypes, respectively.

4. Results and discussion

All preparations described in this study yielded polycrystalline products. Fig. 1a shows the PXRD pattern of the product obtained from a cobalt nitrate melt. Urea hydrolysis increases the pH of the medium and Co(II) is expected to precipitate as its hydroxide. β-$Co(OH)_2$ is a well characterized phase (PDF: 30-443) with a basal spacing of 4.6 Å. However, the first reflection in the observed pattern appears at 6.98 Å followed by another at 3.46 Å. All the reflections were indexed to a triple layered rhombohedral cell ($a = 3.182$ and $c = 20.79$ Å). Wet chemical analysis showed this compound to have the formula $Co_3(OH)_4(NO_3)_2$ (Table 1). All the lines in the powder pattern also match with those reported for $Ni_3(OH)_4(NO_3)_2$ in the literature (PDF: 22-752).

However there is no report of the single crystal structure of either compound.

In such an instance, it is illuminating to describe the overall structure of the solid in terms of the packing of anions. Using symbols A, B and C to represent hydroxyl ion positions and symbols a, b and c to represent cation positions, the metal hydroxide slab, $[M(OH)_2]$ can be represented by the symbol AbC or more simply as AC. The brucite-like structure would then comprise a hexagonal stacking of these slabs as AC AC AC–. We use the nomenclature of Bookin and Drits [25] to characterize this stacking sequence as 1H. '1' denotes the single layered periodicity and 'H' stands for the hexagonal stacking. Other stacking sequences are possible. Three distinct stacking sequences are envisaged for a structure with a two-layer periodicity [25]:

(i) AC CA AC----$2H_1$
(ii) AC AB AC----$2H_2$
(iii) AC BA AC----$2H_3$

Of these, the $2H_1$ polytype generates only prismatic interlayer sites, the $2H_2$ generates only octahedral interlayer sites, while the $2H_3$ polytype generates an equal number of prismatic and octahedral interlayer sites. Structures with three-layer periodicity having the rhombohedral symmetry can be generated by only two sequences:

(iv) AC CB BA AC—$3R_1$
(v) AC BA CB AC—$3R_2$

The $3R_1$ polytype generates only prismatic interlayer sites, while the $3R_2$ generates only octahedral interlayer sites. Within the rhombohedral symmetry, different polytypes have same cell dimensions, number of layers per unit cell and peak positions. The only way to distinguish one polytype from the other is to examine the relative intensities of different reflections.

The Bragg reflections of a hexagonal layered compound belong to the following types:

(1) Basal reflections of the type $0\,0\,\ell$,
(2) The two-dimensional reflections $h\,k\,0$,
(3) $h\,0\,\ell/0\,k\,\ell$ reflections and
(4) $h\,k\,\ell$.

The interlayer spacing depends on the size of the intercalated anion. Within a given range of polytypes, the interlayer spacing remains the same. In a given series of polytypes, the layer remains the same and the structures of different polytypes differ only along the stacking direction, which in crystals of trigonal symmetry also happens to be the *c*-crystallographic axis. Consequently the $0\,0\,\ell$ and the $h\,k\,0$ reflections remain invariant in different polytypes. Only a few general reflections of the type $h\,k\,\ell$ are observed with any significant intensity among the layered hydroxides [25]. Therefore different polytypes can be distinguished from each other only by the relative intensities of the $h\,0\,\ell/0\,k\,\ell$ reflections. These reflections are the only indicators of specific stacking sequences of different polytypes [16]. DIFFaX simulations are very useful for the qualitative estimation of the relative intensities of the $h\,0\,\ell/0\,k\,\ell$ reflections [22,23].

The $h\,0\,\ell/0\,k\,\ell$ reflections appear in the mid. -2θ region (30–50° 2θ; 2.7–1.8 Å) of the PXRD pattern. The prominent reflections characteristic of different polytypes are listed in Table 2. Figs. 1b and c show the DIFFaX simulated PXRD patterns of the $3R_2$ and $3R_1$ polytypes, respectively, of cobalt hydroxynitrate. As expected, the simulated powder X-ray diffraction patterns of $3R_1$ and $3R_2$ polytypic modifications are very similar except for the differences in the relative intensities of the $h\,0\,\ell/0\,k\,\ell$ family of reflections. While the *1 0 1*, *1 0 4* and *1 0 7* reflections are intense in the $3R_2$ polytype, the *0 1 2*, *0 1 5* and *0 1 8* reflections are intense in the $3R_1$ polytype. It is qualitatively clear from the observed intensities of the *1 0 1*, *1 0 4* and *1 0 7* reflections relative to those of the *0 1 2*, *0 1 5* and *0 1 8* reflections (Fig. 1a), that the cobalt hydroxynitrate crystallizes in the $3R_2$ rather than the $3R_1$ polytypic form. The mismatch between the observed and simulated relative intensities of the basal reflections is due to the exclusion of the interlayer species in the model simulations [22].

When the cobalt hydroxynitrate is aged in the tartarate buffer, the nitrate ions are exchanged for the tartarate ions. The PXRD pattern of the resultant compound also shows

Table 2
A comparison of the observed *d*-spacings in the mid. -2θ region with the calculated values corresponding to different $h\,0\,\ell/0\,k\,\ell$ reflections of the three-layer polytypes

$h\,k\,\ell$	$Co_3(OH)_4(NO_3)_2$			$Co_3(OH)_4(C_4H_6O_6)\cdot 3.9H_2O$			α-cobalt hydroxide		
	d (Å)			*d* (Å)			*d* (Å)		
	Obs.	$3R_1$	$3R_2$	Obs.	$3R_1$	$3R_2$	Obs.	$3R_1$	$3R_2$
1 0 1	2.72		2.73			2.65			2.68
0 1 2		2.66		2.60	2.60		2.63	2.63	
1 0 4	2.43		2.43			2.42			2.45
0 1 5		2.29		2.30	2.30		2.33	2.33	
1 0 7	2.02		2.01			2.07			2.09
0 1 8		1.890		1.95	1.95		1.98	1.98	

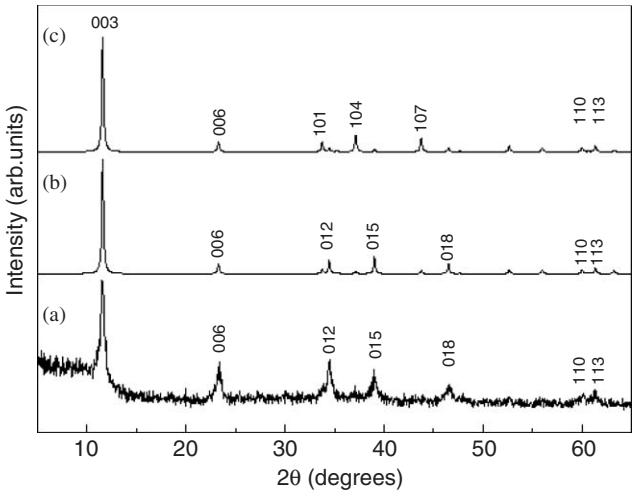

Fig. 2. (a) Observed PXRD pattern of cobalt hydroxytartarate compared with the DIFFaX simulated patterns of (b) $3R_1$ and (c) $3R_2$ polytypes, respectively.

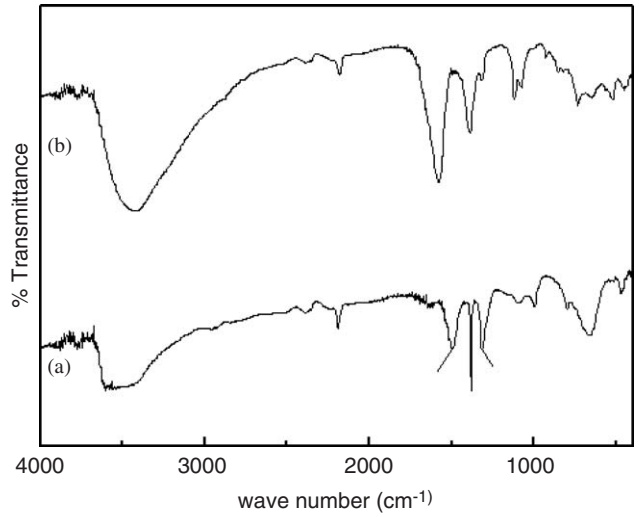

Fig. 3. Infrared spectra of (a) cobalt hydroxynitrate and (b) cobalt hydroxytartarate.

the characteristics features of rhombohedral symmetry (Fig. 2a). The interlayer spacing has increased from 6.98 to 7.6 Å with another peak observed at 3.83 Å. The sharp lines in the mid. -2θ region (2.7–1.8 Å) are retained even in the aged sample indicating an ordered stacking sequence. Figs. 2b and c show the simulated PXRD patterns for $3R_1$ and $3R_2$ polytypes, respectively. The intensities of *0 1 2*, *0 1 5* and *0 1 8* reflections are high relative to the *1 0 1*, *1 0 4* and *1 0 7* reflections in the observed pattern. This matches with the pattern simulated for the $3R_1$ polytype. It is evident that anion exchange results in the transformation of $3R_2 \rightarrow 3R_1$ polytype. It is clear that despite having a common planar geometry, the NO_3^- ion prefers the $3R_2$ polytype, while the carboxylate prefers the $3R_1$ polytype.

In Fig. 3 are shown the infrared spectra of the cobalt hydroxynitrate and the cobalt hydroxytartarate. The two samples show broad bands in the high wave number (3700–3000 cm^{-1}) region due to hydrogen bonded OH groups. There is an absorption at 2190 cm^{-1} due to the isocyanate ion (NCO^-), which is one of the products of urea hydrolysis, and therefore can be expected to be included in the interlayer region during synthesis. In the low wave number (800–400 cm^{-1}) region are seen bands due to the δ(Co–O–H) (669 cm^{-1}) and ν(Co–O) (478 cm^{-1}) vibrations. The bands due to the nitrate groups are seen in the 1600–1000 cm^{-1} region. The as-prepared cobalt hydroxynitrate shows four strong absorptions. Three of these (ν_1: 1321 cm^{-1}; ν_3: 1000 cm^{-1} and ν_4: 1507 cm^{-1}) have been assigned to the strongly bound nitrate group while the fourth (ν_2: 1393 cm^{-1}) arises due to the interaction of the sample with the KBr in the pellet. The large splitting $\Delta\nu$, 180 cm^{-1}, between the ν_4 and ν_1 vibrational modes of the nitrate ion in the IR spectrum of cobalt hydroxynitrate reveals that one of the oxygen atoms of the nitrate group is directly coordinated to the metal atom to complete the octahedral coordination around the metal ion [26,27]. Therefore the nitrate is bound directly to the metal ion through strong covalent bonding. This kind of coordination is termed as 'grafting' [28]. Enthalpy minimization takes place due to the completion of the first coordination shell around the metal ion during the crystallization process. This results in the lowering of the free energy of the crystal. In this mode of coordination, one of the C_2 axes (N–O) of the nitrate ion is parallel to the *c*-crystallographic axis. Following Halford's rules [29], the symmetry of the coordinated nitrate ion is C_{2v} and the IR spectrum has all the signatures of this lower symmetry.

The tartarate intercalated sample displays the asymmetric (ν_{as}) and symmetric (ν_s) COO^- stretches of the carboxylate anion at 1579 and 1393 cm^{-1}, respectively. The $\Delta\nu$ splitting between the ν_{as} and ν_s provides information about coordination of the carboxylate to the metal ion in the layer [30].

The observed dissolution of the cobalt hydroxynitrate in the tartarate buffer clearly indicates that anion exchange takes place by the dissolution-reprecipitation mechanism. The anion exchange reaction is an activity driven process. In case of tartarate exchange the reaction is exothermic owing to the higher negative charge of the tartarate ion compared to the nitrate. Therefore cobalt hydroxynitrate dissolves and reprecipitates in the presence of the dicarboxylate anion to form tartarate-intercalated cobalt hydroxy salt. During the reprecipitation the symmetry and the geometric features of the incoming anion play a crucial role resulting in the $3R_2 \rightarrow 3R_1$ transformation.

In Fig. 4 are shown the thermogravimetric data. Cobalt hydroxynitrate decomposes in a single step at 290 °C, deanation and dehydroxylation takes place simultaneously leading to the formation of Co_3O_4. The single step weight loss (observed: 37.5%, expected: 34.0%) here is consistent with the absence of any intercalated water. The mismatch between the observed and expected losses is probably due

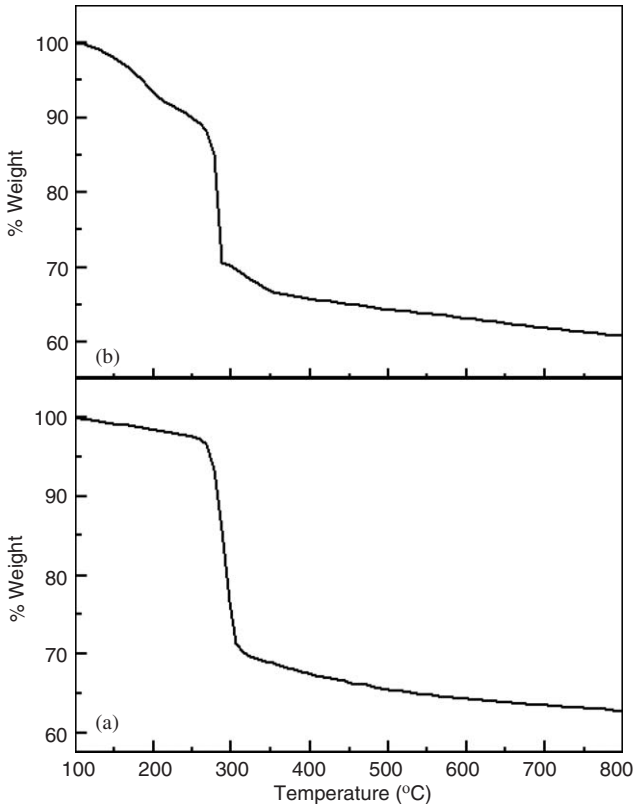

Fig. 4. Thermograms of (a) cobalt hydroxynitrate and (b) cobalt hydroxytartarate, respectively.

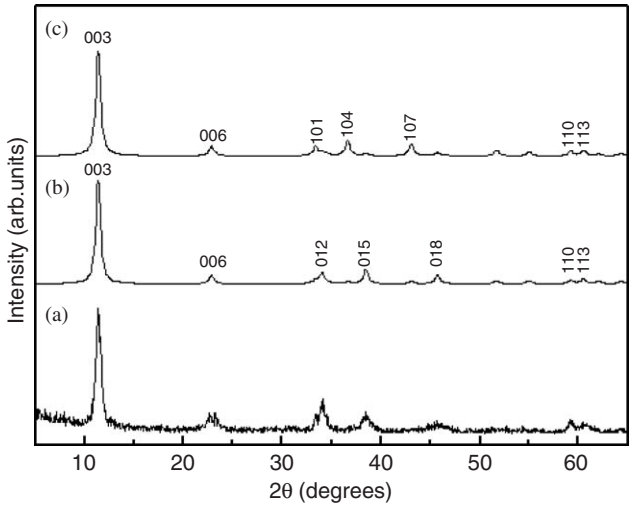

Fig. 5. Observed PXRD pattern of α-cobalt hydroxide compared with the DIFFaX simulated patterns of (b) $3R_1$ and (c) $3R_2$ polytypes, respectively.

to intercalated cyanate ions. The cobalt hydroxytartarate, on the other hand, exhibits two overlapping mass losses. The first loss is observed in the range 100–220 °C (8.0%) and the second loss is observed around 220–800 °C (31.5%). The total mass loss (39.5%) matches with what is expected from chemical analysis (39.3%) (see Table 1). Chemical analysis indicates the presence of intercalated water consistent with the altered mode of carboxylate intercalation compared to the nitrate. The carboxylates prefer to be intercalated with their plane parallel to the metal hydroxide slabs [31]. The symmetry of coordination would be D_{3h}. The D_{3h} symmetry maximizes the H-bonding between the carboxylates and the metal-hydroxide slabs. But this mode of intercalation does not satisfy the coordinative unsaturation of the metal ion, necessitating the inclusion of coordinated water molecules.

To investigate the effect of intercalated chloride, two routes were explored for the synthesis of the cobalt hydroxychloride. In the first route cobalt hydroxynitrate was subjected to anion exchange for Cl^- in a sodium chloride solution. The resulting compound has $x = 0.22$ which is much less than the typical values (0.5–1.0) seen in basic salts. This hydroxyl-rich composition is associated with the α-hydroxides [32,33]. The α-hydroxides are obtained by the protonation of a fraction, x, of the hydroxyl ions. The chloride ion is outside the first coordination shell of the cation and the resultant formula is $[Co(OH)_{1-x}(H_2O)_x]Cl_x$ ($x = 0.22$). The α-hydroxides differ from the basic salts in the mode of bonding of the intercalated anions [34]. The PXRD pattern of α-cobalt hydroxide is shown in Fig. 5a. The 0 0 6 reflection is broadened due to incomplete anion exchange resulting in interstratification [19] while the peaks in the mid. -2θ are broadened due to the presence of stacking faults. Nevertheless, all the reflections observed could be indexed to rhombohedral symmetry. The interlayer spacing has increased from 6.98 to 7.82 Å indicating that the Cl^- ion is outside the first coordination shell. Simulated PXRD patterns for $3R_1$ and $3R_2$ are shown in Figs. 5b and c. It is clear that the peak positions and peak shapes of 0 1 2, 0 1 5, 0 1 8 match qualitatively with the observed pattern indicating that chloride intercalated α-cobalt hydroxide crystallizes in the $3R_1$ polytype clearly showing the preference of Cl^- ions for the $3R_1$ polytype (Table 2).

In the second route, the cobalt hydroxychloride was synthesized directly from $CoCl_2$ by urea hydrolysis. Fig. 6a shows the PXRD pattern of cobalt hydroxychloride. This pattern is different from those of the other salts. All the reflections could be matched with those reported for the compound $Co_2(OH)_3Cl$ ($x = 0.5$) in the literature. The single crystal structure of this compound has been reported (ICSD: 24685). All the reflections were indexed to a rhombohedral cell ($a = 6.808$ Å; $c = 14.558$ Å) (Table 3) in keeping with the literature [35]. To determine the specific polytype, DIFFaX simulations of the PXRD patterns were carried out (see Figs. 6b and c). The observed pattern of $Co_2(OH)_3Cl$ matches with the simulated PXRD pattern of the $3R_1$ polytype showing that the Cl^- ion selects for the $3R_1$ polytype.

Fig. 7 shows the PXRD pattern of cobalt hydroxysulfate and all the reflections are considerably broadened. This pattern displays a low angle reflection at 7.92 Å attributed to *0 0 3* and an asymmetric 'saw-tooth' line shape in mid.

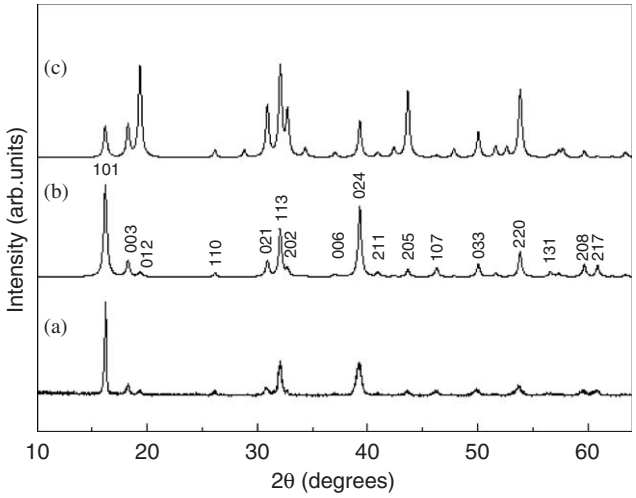

Fig. 6. Observed PXRD pattern of cobalt hydroxychloride compared with the DIFFaX simulated patterns of (b) $3R_1$ and (c) $3R_2$ polytypes, respectively.

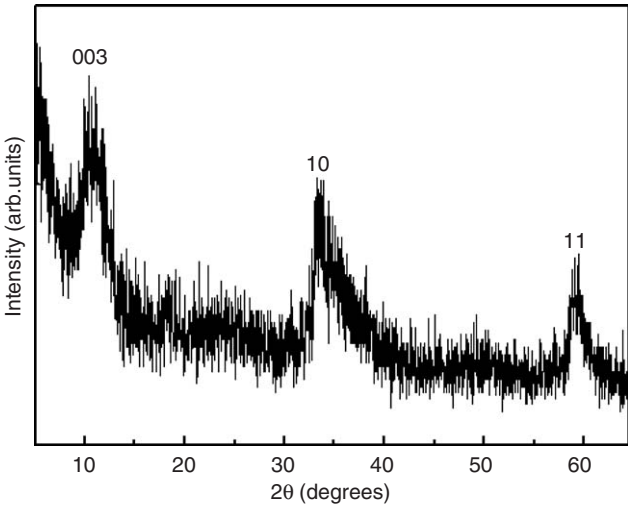

Fig. 7. PXRD pattern of cobalt hydroxysulphate.

Table 3
A comparison of the observed *d*-spacings of $Co_2(OH)_3Cl$ with the values calculated for the $3R_1$ polytype

hkℓ	Sample *d*(obs) (Å)	$3R_1$ polytype *d*(cal) (Å)
101	5.47	5.46
003	4.85	4.85
012	4.58	4.58
110	3.40	3.40
021	2.90	2.88
113	2.79	2.78
202	2.74	2.73
006	2.43	2.42
024	2.29	2.29
211	2.20	2.20
205	2.07	2.07
107	1.96	1.96
033	1.82	1.82
220	1.70	1.70
131	1.63	1.62
208	1.55	1.54
217	1.52	1.52

-2θ region. This kind of asymmetric line broadening arises due to the loss of registry between the successive layers—a phenomenon known as tubrostraticity. A turbostratically disordered material has no three-dimensional periodicity, resulting in the extinction of all $hk\ell$ reflections. However the electron density is periodic along the stacking direction, resulting in the 00ℓ reflections. Each layer is however ordered and generates two-dimensional reflections, hk, which acquire a 'saw tooth' line shape [36,37]. The turbostratic disorder is a direct consequence of the mismatch between the crystallographically defined interlayer sites generated within a crystal with rhombohedral symmetry and the tetrahedral symmetry of the SO_4^{2-} ions. Due to the mismatch the SO_4^{2-} ions are unable to anchor the metal hydroxide slabs in an ordered stacking sequence.

5. Conclusion

We conclude that different hydroxysalts of Co(II) crystallize in structures corresponding to different polytypes. Polytype selectivity is exercised by the corresponding anions and their mode of intercalation. Anions coordinating in the C_{2v} symmetry select for the $3R_2$ polytypes, while anions coordinating in D_{3h} symmetry select for $3R_1$. Anions of tetrahedral symmetry produce turbostratic disorder.

Acknowledgments

P.V.K. thanks the Department of Science and technology, Government of India (GOI) for financial support. T.N.R. thanks the Council of Scientific and Industrial Research, GOI for the award of a Senior Research Fellowship (NET). Authors thank the Solid State and Structural Chemistry Unit, Indian Institute of Science for powder X-ray diffraction facilities.

References

[1] H.R. Oswald, R. Asper, in: R.M.A. Leith (Ed.), Preparation and Crystal Growth of Materials with Layered Structure, Riedel Publishing Company, Netherlands, 1977.
[2] P.M. Louer, L. Grandjean, Acta Crystallogr. B 29 (1973) 1696.
[3] M. Meyn, K. Beneke, G. Lagaly, Inorg. Chem. 32 (1993) 1209.
[4] H. Nishizawa, L. Markov, R. Ioncheva, J. Mater. Sci. Lett. 141 (1998) 229.
[5] D. Louer, J. Solid State Chem. 13 (1975) 319.
[6] P. Gallezot, M. Prettre, Bull. Soc. Chim. Fr. (1969) 407.
[7] M. Louer, D. Louer, D. Grandjean, D. Weigel, Acta Crystallogr. B 29 (1973) 1707.
[8] L. Markov, K. Petrov, V. Petrov, Thermochim. Acta 106 (1986) 283.

[9] K. Petrov, N. Zotov, O. Garcia-Martinez, R. Rojas, J. Solid State Chem. 101 (1992) 145.
[10] L. Eriksson, D. Louer, P.E. Werner, J. Solid State Chem. 81 (1989) 9.
[11] M. Rajamathi, P.V. Kamath, Int. J. Inorg. Mater. 3 (2001) 901.
[12] A.F. Wells, Structural Inorganic Chemistry, Oxford University Press, Oxford, 1979.
[13] V.R. Allmann, Z. Kristallogr 126 (1968) 417.
[14] R. Prasad, O.N. Srivastava, J. Appl. Crystallogr. 4 (1971) 516.
[15] A.M. Fogg, A.J. Freij, G.M. Parkinson, Chem. Mater. 14 (2002) 232.
[16] S.P. Newman, W. Jones, P. O'Connor, D.N. Stamires, J. Mater. Chem. 12 (2002) 153.
[17] A.R. Verma, P. Krishna, Polymorphism and Polytypism in Crystals, Wiley, New York, 1966.
[18] S.P. Newman, W. Jones, J. Solid State Chem. 148 (1999) 26.
[19] T.N. Ramesh, P.V. Kamath, C. Shivakumara, J. Electrochem. Soc. 152 (2005) 806.
[20] A.V. Radha, P.V. Kamath, G.N. Subbanna, Mater. Res. Bull. 38 (2003) 731.
[21] M.M.J. Treacy, M.W. Deem, J.M. Newsam, Computer Code DIFFaX, Version 1.807, 2000.
[22] G.S. Thomas, M. Rajamathi, P.V. Kamath, Clays Clay Miner. 52 (2004) 693.
[23] A.V. Radha, C. Shivakumara, P.V. Kamath, Clays Clay Miner. 53 (2005) 521.
[24] C. Tessier, P.H. Haumesser, P. Bernard, C. Delmas, J. Electrochem. Soc. 146 (1999) 2059.
[25] A.S. Bookin, V.A. Drits, Clays Clay Miner. 41 (1993) 551.
[26] F. Portemer, A. Delahaye-Viadal, M. Figlarz, J. Electrochem. Soc. 139 (1992) 671.
[27] P. Rabu, S. Angelov, P. Legoll, M. Belaiche, M. Drillon, Inorg. Chem. 32 (1993) 2463.
[28] V.R.L. Constantino, T.J. Pinnavaia, Inorg. Chem. 34 (1995) 883.
[29] S.D. Ross, Inorganic Infrared and Raman Spectra, McGraw-Hill, London, 1972.
[30] J. Zhang, F. Zhang, L. Ren, D.G. Evans, X. Duan, Mater. Chem. Phys. 85 (2004) 207.
[31] V. Prevot, C. Forano, J.P. Besse, J. Mater. Chem. 9 (1999) 155.
[32] M. Rajamathi, P.V. Kamath, R. Seshadri, Mater. Res. Bull. 35 (2000) 271.
[33] Z. Liu, R. Ma, M. Osada, K. Takada, T. Sasaki, J. Am. Chem. Soc. 127 (2005) 13869.
[34] M. Rajamathi, P.V. Kamath, J. Power Sources 70 (1998) 118.
[35] P.M. de Wolff, Acta Crystallogr. 6 (1953) 359.
[36] Y.G. Andrew, T. Lundstrom, J. Appl. Crystallogr. 27 (1994) 767.
[37] B.E. Warren, P. Bodenstein, Acta Crystallogr. 20 (1966) 602.